Received 1 March 2019
Revised 19 June 2019
26 June 2019
28 June 2019
Accepted 29 June 2019

Development of femoral component design geometry by using DMROVAS (design method requiring optimum volume and safety)

Burak Öztürk
Bilecik Seyh Edebali University, Bilecik, Turkey, and

Fehmi Erzincanli
Duzce Universitesi, Duzce, Turkey

Abstract

Purpose – This study aims to design a femoral component with minimum volume and maximum safety coefficient. Total knee prosthesis is a well-established therapy in arthroplasty applications. And in particular, with respect to damaged or weakened cartilage, new prostheses are being manufactured from bio-materials which are compatible with the human body to replace these damages. A new universal method (design method requiring optimum volume and safety [DMROVAS]) was propounded to find the optimum design parameters of tibial component.

Design/methodology/approach – The design montage was analyzed via the finite element method (FEM). To ensure the stability of the prosthesis, the maximum stress angle and magnitude of the force on the knee were taken into consideration. In the analysis process, results revealed two different maximum stress areas which were supported by case reports in the literature. Variations of maximum stress, safety factor and weight were revealed by FEM analysis, and ANOVA was used to determine the F force percentage for each of the design parameters.

Findings – Optimal design parameter levels were chosen for the individual's minimum weight. Stress maps were constructed to optimize design choices that enabled further enhancement of the design models. The safety factor variation (SFV) of 5.73 was obtained for the volume of 39,219 mL for a region which had maximum stress. At the same time, for a maximum SFV and at the same time an average weight, values of 37,308 mL and 5.8 for volume and SFV were attained, respectively, using statistical methods.

The authors would like to thank the Düzce University Scientific Research Unit (DÜ-BAP) for their support of the project titled "Optimization of Design Geometry in Arthroplasty BioEngineering Materials, Fracture Analysis, Investigation of Mechanical and Microstructural Properties."

Compliance with ethical standards

Funding: The research on the optimization of total knee prosthesis assembly parts has been financed by Duzce University Scientific Research Department with the project number 2018.06.05.728.

Ethical approval: This article does not contain studies with animals performed by any of the authors. This article does not contain studies with human participants or animals performed by any of the authors.

Conflict of interest: Author Öztürk and Erzincanli were supported by a scientific research project by Düzce University.

Engineering Computations
Vol. 37 No. 2, 2020
pp. 682-704

0264-4401
DOI 10.1108/EC-03-2019-0077

Originality/value – This proposed optimal design development method is new and one that can be used for many biomechanical products and universal industrial designs.

Keywords Parametric design, Total knee prosthesis, Arthroplasty, Design optimization method, Femoral component

Paper type Research paper

1. Introduction

Various prosthetic applications can be used to compensate for the damage to cartilage tissue caused by diverse health problems. Knee prostheses are made from bio-materials compatible with human body tissue and include three main parts: the tibial component, the femoral component and the ultra-high molecular weight polyethylene (UHMWPE) insert between the two. However, these implants can be damaged as a result of time-related changes in patient weight, insufficiency of material microstructure, fatigue and wear. One recognized treatment for unilateral osteoarthritis occurring in the knee was unicompartmental knee arthroplasty (UKA). This procedure has been performed since the early 1970s, although initial results were found to be inconsistent (Laskin, 1978; Insall and Aglietti, 1980). However, improved design and surgical techniques, as well as patient preferences, have given rise to better UKA performance and survival rates. Survival is currently taken to mean that the osteoarthritis has not spread to other joint compartments and that no loosening of the implant has occurred (Borus and Thornhill, 2008). Although the average lifespan of a prosthesis is fifteen years, knee prostheses may become unusable much earlier than expected because of such reasons (Luring *et al.*, 2007; Wada *et al.*, 1997; Cameron and Welsh, 1990; Sandborn *et al.*, 1987; Van der Veen and Van Raay, 2014; Panousis *et al.*, 2004; Boran *et al.*, 2005). A relationship exists between material fatigue and the weight of the patient. One patient gained 38 per cent more weight after arthroplasty. The weight gain surgeons observed on their patient had caused fatigue wear on his prosthesis and accordingly, fracture occurred. In addition, the sharp bend and thin metal (4 mm) in the design were subjected to continuous load and this caused regions of high stress concentration. Nearly nine years after the first arthroplasty, the patient underwent repair surgery for the broken prosthesis [Figure 1(a)] (Luring *et al.*, 2007).

Research was carried out and three cases were found with stress fractures of the femoral component in knee arthroplasty 32, 52 and 73 months after repair surgery. The most probable cause of failure was owing to the thinness of the metal in this design area

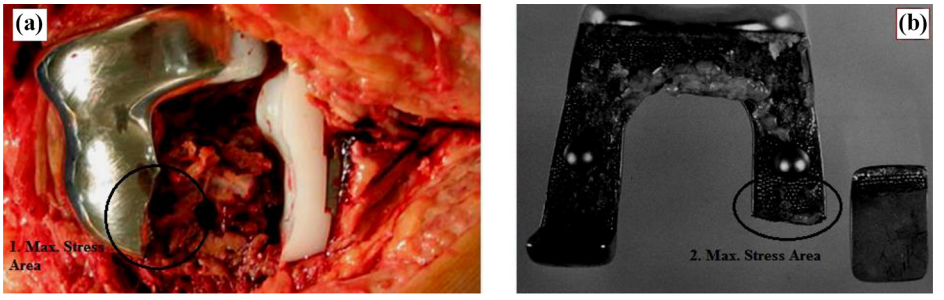

Figure 1. Fractured femoral components

Sources: Luring *et al.* (2007); Wada *et al.* (1997)

[Figure 1(b)] (Wada *et al.*, 1997). Figure 1 shows pictures of the maximum stress areas of two different regions of different products.

It has been reported in the literature that fractures of femural components are caused by design and metallurgical problems. A fracture of the anterior flange of a femoral component in a knee has been seen. This was thought to be because of lack of bony support leading to cantilever bend. The solution would seem to be to add a metal web to strengthen that area of the femoral component (Cameron and Welsh, 1990). Following 11 years *in situ*, the knee implant was removed. Femoral component had fractured 1 cm from the anterior edge. The factors contributing to the mechanical failure of the implant and to its clinical intolerance were examined. The factors that raised tensile stresses were found to include improper surgical placement and wear on the weight-bearing surface of the component, together with the quality of the implant material (Sandborn *et al.*, 1987). All these factors were blamed on older designs, in particular uncemented models. Thus, poor design, improper implant placement and loosening had led to increase stress and subsequent wear which resulted in the breakage of the component (Van der Veen and Van Raay, 2014). However, design failures owing to poor resistance and material specifications have also been reported concerning the tibial component and polyethylene insert (Panousis *et al.*, 2004; Boran *et al.*, 2005). The breakdown mechanism of the prostheses was linked to polyethylene wear and as a result, more than half of the prosthesis designs were modified (Panousis *et al.*, 2004). Excessive polyethylene wears, osteolysis, metallurgical weakness in the internal structure and some design characteristics of the tray have been identified as factors contributing to implant failure these results indicate that problems such as design and metallurgical weakness may arise in the tibial component (Boran *et al.*, 2005). The life expectancy of a prosthesis is fifteen years according to the literature, despite the fact that different types of fractures have occurred earlier in total knee prostheses (TKP) (Luring *et al.*, 2007; Wada *et al.*, 1997; Cameron and Welsh, 1990; Sandborn *et al.*, 1987; Van der Veen and Van Raay, 2014; Panousis *et al.*, 2004; Boran *et al.*, 2005). Generally, the results of the literature surveys showed that errors in design geometry and weight gain over time caused these breaks. Insufficient wall thickness in curves and stress areas constitutes the basic design geometry problem. All these findings indicate that the number of optimization studies conducted for design geometry is inadequate. In the literature, researchers have investigated the methods used to measure TKP and have presented new methods to determine the optimum design geometry for minimum volume.

Belted design geometry in the stress areas was developed to prevent industrial design problems in pipe fittings (Küçük and Öztürk, 2017a, 2017b). Volume, safety factor and maximum strain variations were investigated using the Taguchi method and FEM for different parameters and levels of this design geometry. The maximum safety factor was determined for the minimal volume (Küçük *et al.*, 2017).

These studies only increased the evaluation options of classical FEM. In this article, the researchers have developed all the missing processes, inspired by the design development method they have previously proposed and consequently identified a new type of method. Using this parametric design method, the TKP would be able to obtain the maximum safety factor for the minimum volume of tibial component products. Moreover, this study has proposed a new optimum design proses which involves the creation of stress distribution maps of the sections with a high amount of stress and investigation of the volume distribution in these regions. As a result of this study, a new universal design development method has been introduced to the literature.

2. Proposed parametric design model to obtain an ideal safety factor

A literature review has revealed the research conducted via finite element analysis (FEA) and product development models related to femoral component optimization (Ilzarbe *et al.*, 2008; Bahraminasab *et al.*, 2014a; Bahraminasab *et al.*, 2014b; Harrysson *et al.*, 2007; Chandran *et al.*, 2009; Huang *et al.*, 2017; Willing and Kim, 2009). Factor levels can be determined that conform to a set of desirable specifications, and steps can be proposed for computational multi-criteria design trials created by design of experiments (DOE) and FEA techniques (Ilzarbe *et al.*, 2008). Multiobjective design optimization of a functionally graded material (FGM) can be applied to a femoral component via FEA and response surface methodology (RSM). Bahraminasab *et al.* presented new mathematical modeling steps to be carried out with RSM. This RSM is the FGM optimal performance and can be used effectively to work out the complex relationship between component design variables and to determine the most responsive parameters affecting FGM properties during the manufacturing phase. The relative performance can be revealed by comparing the use of a standard Co–Cr alloy in a femoral component knee implant with the applied FGM optimization (Bahraminasab *et al.*, 2014a). In addition, Bahraminasab *et al.* examined the influence of material selection and geometric configuration on the performance of the femoral component in a UKA depending on the positioning of the pegs used in the design. Using the analysis tools of advanced computer software, a complex design process was carried out to examine the changes that affect stress shielding, which are among the most prevalent factors leading to UKA failure (Bahraminasab *et al.*, 2014b). Harrysson *et al.* presented a special custom design approach based on a computed tomography (CT) scan of the patient's joint. The problems associated with traditional knee implant components were addressed in this design which included customized bone-implant and articulating surfaces. The customized femoral component design was compared with a traditional design using FEA. Premature loosening of the implant may result from uneven remodeling of the bone, which can be reduced by the more even distribution of the stress on the joint provided by the proposed model. The interface between bone and implant at the distal femur is capable of tolerating anatomical abnormalities, thus reducing the necessity of surgical interventions or insertion of filler components (Harrysson *et al.*, 2007). The design optimization of a UKA presented by Willing and Kim used a parametric 3D FE model which took into consideration the wear of the UHMWPE insert. The wear on the insert was decreased by 18.5 per cent from 55.248 to 45.013 mm^3 for each year of use. This was achieved by the modification of the contact geometry of the frontal and sagittal planes of both components. The radius of the curvature of the femoral condyle in the sagittal plane was reduced, whereas the radius in the frontal plane was increased, thus reducing the fit between the components of the implant (Chandran *et al.*, 2009). To examine the contact characteristics, two designs were selected by Huang *et al.* An anatomical V-shaped design (VSD) and a dome-shaped design (DSD) were chosen for the anterior trochlear surface of a novel femoral component. They simulated the use of resurfaced and unresurfaced patellae. The distribution of stress and strain on the patellar bone was calculated and compared. Without patellar resurfacing, the maximum compressive strain on the patellar bone in the VSD model was about 20 per cent lower than in the DSD model.

However, with patellar resurfacing, the maximum strain was 13.3 per cent higher in the VSD model than in the DSD model (Huang *et al.*, 2017). In the literature a number of optimization studies are also available on modeling by changing the width, size, angle, etc. of TKP design geometry (Willing and Kim, 2009; Dai *et al.*, 2014; Van den Heever *et al.*, 2011; Kumar and Sarkar, 2018). Chandran *et al.* aimed to optimize the design of femoral cam-tibial post articulation using FEA and proposed various design parameters to optimize femoral

roll-back. Femoral roll-back and pressure distribution of the tibial post are indicated in the results. Small design modifications to the tibial post resulted in major changes in the femoral roll-back, accompanied by comparatively small increases in contact pressure at the tibial post (Willing and Kim, 2009). A multi-ethnic dataset which included Caucasian, Indian, and Korean patients was used by Dai *et al.* to investigate component fit in six groups of contemporary femoral component design. The component overhang/underhang between the resected distal femur and the size of the corresponding component were measured and compared among designs and ethnic groups. For the entire dataset and for each ethnicity, the degree of overhang/underhang and the tendency to downsize because of clinically significant overhang were calculated. This study found variable levels of morphological conformity for six current femoral designs for total UKA. The data indicated that the design of femoral components presenting a large number of medial lateral/anterior posterior (ML/AP) shapes in an increasing number of sizes may enable essential selection of the component to sufficiently fit the resected femur of the investigated ethnic groups without clinically significant overhang (Dai *et al.*, 2014). Van den Heever *et al.* proposed a technique that allows preoperative identification of the most appropriate type and size of the prosthesis to be used in a specific patient subjected to knee replacement surgery. An unsupervised neural network was used to estimate the parameters of healthy knee geometry and these were then applied in a goodness of fit (GoF) test to identify which type and size of femoral a prosthesis was the best fit. This method was applied in the determination of the most appropriate of three implants for 34 different patients. This approach demonstrates the potential of helping surgeons in the selection of the optimal size and type of prosthesis from among the range of conventional UKA (Van den Heever *et al.*, 2011). In view of the increasing demand for UKA, Kumar and Sarkar proposed the material-model for the practical and effective optimization of UKA. In this study, various computer-aided design (CAD) models of knee prostheses using metals, ceramics and polymers were presented, and the best material-model in terms of function and life span was determined. When features of design, dimension and material were considered, the ZTA-based double stem with base connector (DSBC) femur, UHMWPE articulating insert and ZTA tibial combination exhibited a higher level of performance under compressive load. The optimized material-model combination enhanced the functional capabilities and consequently, was expected to reduce the need for resection among younger patients (Kumar and Sarkar, 2018). In addition, researches on various model designs are also available in different types of research (Minnoye and Plettenburg, 2009; Vertullo *et al.*, 2018). This study has attempted to create the ideal knee prosthesis design geometry. Researchers have indicated that optimum design could only be achieved with a minimum volume and a maximum safety factor value; however, the parameters that make up a design and the effects of different measurements on strength properties have not been investigated in other studies. The effect rates of each design parameter on strength and volume variations are determined. If desired, validation analyses can be performed using a number of methods. In the last step, the main criteria for the design are determined. The optimum design geometry is obtained according to these criteria.

3. Materials and methods

In this new model for optimization of the design geometry of TKPs, some auxiliary software and methods were used. Different types of design geometries were modeled with the help of the Solid Works 2015 Computer-Aided Design (CAD) program for the experimental FEA with the help of the ANSYS 19.2 Computer-Aided Engineering (CAE) program. In this study, the Taguchi method was used for the design of the experiment and ANOVA for the

effect intensity of the design parameters via the Minitab 18. Program. This method consisted of a total of nine processes with three main steps.

4. The proposed methodology: design method requiring optimum volume and safety

This proposed method consists of three main steps and nine sub-steps. When applying this method, first, the ideal design model is selected and then the design parameters that make up this design model are determined. These determined design parameters are adjusted according to the minimum and maximum measurement range. In the second step, the variations in the design range of each design parameter change the strength calculations and volume amount by a specific ratio. The effects of the variations between the levels of each parameter on the results can be calculated using different statistical methods. Conditions for FEA and other statistical analyses are then determined. As a result of the analytical studies and calculations, in some optimum design studies it may be desirable to have a minimum volume, while in others it is desirable to obtain a maximum safety factor. For such different criteria, statistical results are re-analyzed, and strength and volume variations are compared. As a result, optimum design geometry can be obtained for the determined engineering stresses and analysis conditions. The three main steps along with the sub-steps of this method are shown in Figure 2. Although this method has been used for a TKP femoral component, it can be applied to develop different industrial designs and bio-engineering materials.

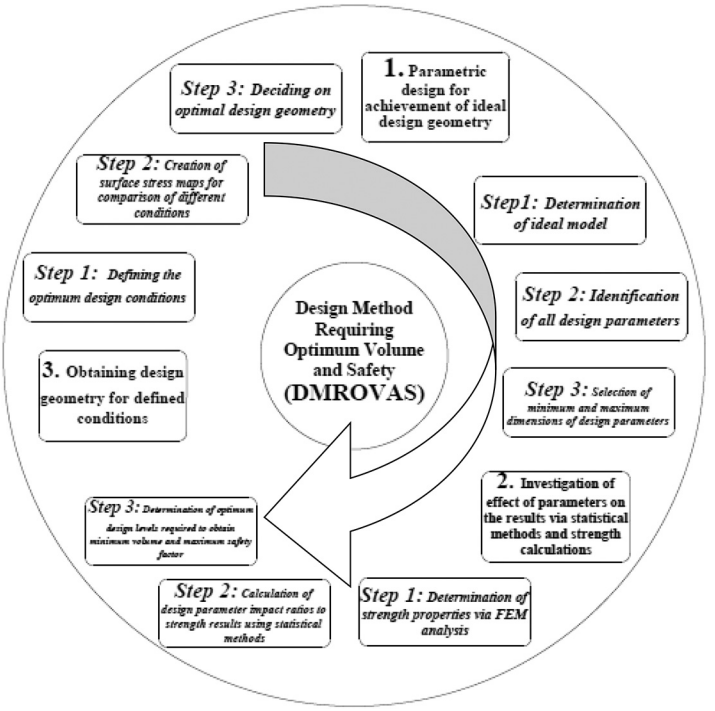

Figure 2.
New industrial design model process

4.1 Parametric design for achievement of ideal design geometry

In the first step of this proposed model, the geometry type was selected and developed as the ideal model for the different design types of the product to be optimized in industrial design. In this process, the criteria used in geometry selection were defined, and the properties of the selected geometry discussed. Many of the CAD programs perform modeling according to a process called the element tree or family tree. During the design of a geometry, each part of the design model is shaped with the help of multiple design tools. Secondly, the different parameters defined in the element tree are determined to form the entire selected geometry type. Finally, the minimum and maximum measurement range of each design parameter is determined within the limits of the design geometry. This geometry may be applied in the industrial field and may exhibit the kinematic and mechanical properties expected from it. An industrial design geometry identification card is prepared in this first step. In other words, the difference of design geometry is explained in the identification card by describing other geometries. Moreover, each design parameter that constitutes this geometry and the measurement range of these parameters is indicated.

4.1.1 Step1: determination of ideal model. Since the first implants were performed in the early 1970s, UKA has been the treatment of choice for unilateral osteoarthritis of the knee (Laskin, 1978; Insall and Aglietti, 1980). Since their early application, TKPs have been produced in many different industrial design geometries and dimensions. The customized design presented by Harrysson *et al.* based on a CT scan of the patient's joint addressed one of the most frequently encountered problems with conventional knee-implant components by customizing both the articulating surface and the bone-implant interface. This new approach for TKP design has led to the possibility of many different design geometries (Harrysson *et al.*, 2007). The two designs selected by Huang *et al.* (VSD and DSD) were chosen for the anterior trochlear surface of a modern femoral component. Dai *et al.* reported six differences in arthroplasty using the aspect ratio (ML/AP) changes for TKP industrial design types (Dai *et al.*, 2014). Apart from those mentioned in these studies, many different design types have been produced according to different design criteria. In this study, to create the simplest design geometry for minimum weight, an applied and kinematic standard design geometry type was selected (Öztürk *et al.*, 2018), as shown in Figure 3.

4.1.2 Step 2: identification of all design parameters. A rectangular box design can be used to describe a design parameter that forms design geometry. A rectangular box design consists of width, length and height (Figure 4). Each design parameter change affects the moment of inertia and amount of weight.

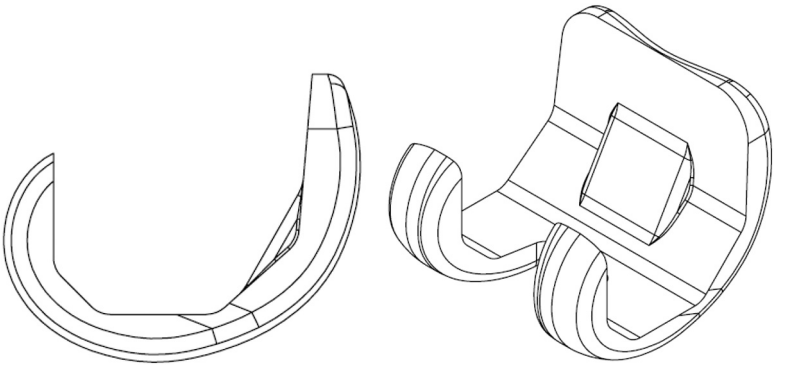

Figure 3.
Model geometry used in designs of experiment

The minimum height and the maximum length are selected in such figures for minimum weight and maximum safety factor. Special methods may be required to make these designs because they do not have a simple geometrical structure as in an industrial design profile (Harrysson *et al.*, 2007; Huang *et al.*, 2017). Biomechanical tests or FEA are used to evaluate the strength characteristics of the models designed with different parameters (Ilzarbe *et al.*, 2008; Bahraminasab *et al.*, 2014a; Bahraminasab *et al.*, 2014b; Harrysson *et al.*, 2007; Chandran *et al.*, 2009; Huang *et al.*, 2017; Willing and Kim, 2009; Dai *et al.*, 2014; Van den Heever *et al.*, 2011; Kumar and Sarkar, 2018). However, no detailed research has been found that addresses the design parameters and levels required for a TKP design. Dai *et al.* reported some dimensions such as AP sizes, AP increments (mm), ML size offerings per AP and aspect ratio (ML/AP) in a TKP design (Dai *et al.*, 2014). Van den Heever *et al.* also investigated a TKP using similarly dimensioning. These parameters are appropriate and effective for TKP selection according to the patient's bone characteristics, weight and age. As described in the section on the determination of the ideal geometry type, in this study, morphological measurements were chosen for the standard AP, resected posterior condyle (RPC) and anterior posterior box (APBOX).

A total of 18 design parameters constituting the three-dimensional model geometry of this standard design were determined using different methods than in other studies (Figure 5). Likewise, unlike other studies, this study determined the effects of 18 different design parameters on the safety factor and the volume variations.

There are four radii where the TKP is connected to the femur ($P_{1\text{-}4}$). In addition, the features of length (P_{13}) and thickness (P_{18}) are established on the flange. This flange geometry is designed to strengthen the knee prosthesis. This flange is reinforced with four radii on the bottom (P_9) on the top (P_{10}) and two on the sides ($P_{8\text{-}11}$). In addition, the radial wax mold is easier to remove in these regions. Designers demand a minimum number of flat surfaces in an industrial design. In TKP design, it is desirable to have curved working

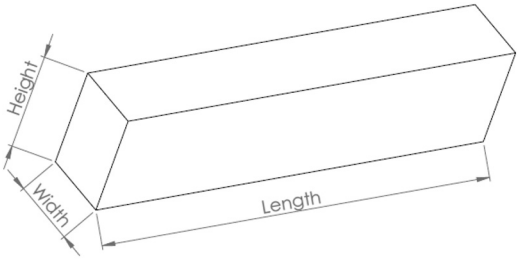

Figure 4.
Design parameters in form of a rectangular box

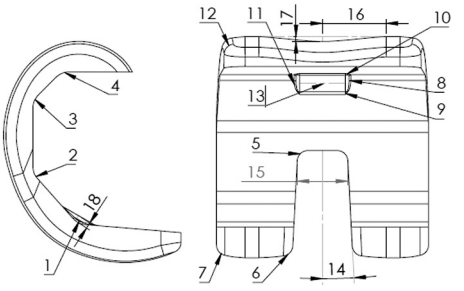

Figure 5.
Femoral component design parameters

surfaces. Therefore, there are two radii in the polyethylene part that is subject to friction ($P_{6\text{-}7}$). Subtraction was performed according to the length (P_{15}) and angle (P_{14}) determined in the area that comes into contact with the curved surface of the polyethylene. In addition, this fork-like recess is reinforced against axial forces by a radius (P_5). Furthermore, the entire upper outline of the radius is formed into a curve (P_{12}). The ellipse-like design, which accommodates the necessary rotational movement of daily activities, is defined by the thickness (P_{17}) and width (P_{16}).

4.1.3 Step 3: selection of minimum and maximum dimensions of design parameters. Each design parameter has a lower and upper measure limit value to provide the desired TKP design. The Taguchi L^{36} mixed ($2^8 \times 3^{10}$) factorial fractional DOE was chosen to investigate the effect of 18 design parameters on strength results. Two levels were selected for the minimum and maximum levels of eight radius measurements.

The other parameters were three levels designed as the lowest, middle and highest values (Table I). Using the Solid Works 2015 CAD program, 36 different industrial design geometries were modeled.

4.2 Investigation of effect of parameters on the results via statistical methods and strength calculations

In the first step, design type, parameters other than morphological measurements and levels of the TKP were defined. By applying statistical methods in the second and third stages of this proposed new model, the effects of each design parameter on strength and volume results were investigated. The ANSYS program used in strength calculations, the FEA, the Taguchi method and ANOVA applications are explained in the intermediate steps.

4.2.1 Step 1: Determination of strength properties via finite element method analysis. Taking into account the literature research, the mechanical properties of the Cr-Co-Mo and UHMWPE materials used in finite element method (FEM) analysis were determined by the ANSYS program material library (Table II). These materials were chosen for the static analysis of engineering stresses (Rawal *et al.*, 2019).

In the literature, the loads applied to a prosthesis during gait have been investigated and it has been determined that these dynamic loads occur at a 45-degree angle on the *z*-axis as a

Table I.
Design parameters for femoral component levels (mm)

Parameters (P)	P_1	P_2	P_3	P_4	P_5	P_6	P_7	P_8	P_9	P_{10}	P_{11}	P_{12}	P_{13}	P_{14}	P_{15}	P_{16}	P_{17}	P_{18}
Levels (L)																		
L_1	5	5	5	5	3	3	3	0.5	4	4	1	6	15	3	14	18	1.5	2
L_2	10	10	10	10	6	6	6	1.5	6	6	1.5	8	20	7	17	20	2	3
L_3	–	–	–	–	–	–	–	–	8	8	2	10	25	10	20	22	2.5	4

Table II.
Mechanical properties of polyethylene insert (UHMWPE) and femoral component (Cr-Co-Mo) used in the analysis

Material	Density (Kg/m^3)	Young's modulus (Pa)	Poisson's ratio	Yield strength (Pa)	Ultimate strength (Pa)
UHMWPE	930	6.90 E+08	0.29	2.10 E+07	4.80 E+07
Cr-Co-Mo	8,300	2.30 E+11	0.3	6.12 E+08	9.70 E+08

result of experimental and finite element studies. These forces were applied at a 3,200 N Fz force and 45° angle to the point where maximum stress occurred and the analysis for stress amount was applied to the knee prostheses. The TKP installation was performed at a 45° angle (Figure 6), the force application surface was fixed to the inner surface of the femoral component (3,200 N) and the tibial component was attached. The analysis was then performed for each design geometry (Villa *et al.*, 2004). The maximum forces involved as determined in the literature were applied via the ANSYS 19.2 CAE program and maximum deformation, maximum stress amount and volume variations were determined for all geometries.

4.2.2 Step 2: calculation of design parameter impact ratios to strength results using statistical methods. Bahraminasab *et al.* applied RSM for their TKP design model (Ilzarbe *et al.*, 2008; Bahraminasab *et al.*, 2014). Response surface methodology is an optimization technique in which the variable-response profile of the system is determined according to the relationship between the independent variables and the responses of the experimental system designed based on these variables (Kibar *et al.*, 2016). The Taguchi method was chosen together with ANOVA for our study because of the high number of parameters. Dr Genichi Taguchi developed his method (Taguchi, 1990) as a tool to determine the optimum combinations of process conditions and today it is extensively applied in the manufacturing and engineering sectors. It is a very powerful instrument for improving high-quality systems design. The Taguchi method allows industries to substantially decrease product development time without increasing the cost (Ross, 1996). The Taguchi method uses an exclusive design of orthogonal arrays to examine the entire parameter space without performing an excessive number of experiments. Orthogonal arrays are used in conjunction with the signal/noise (S/N) ratio in the Taguchi method, whereby the experimental outcomes are transferred to the S/N ratio. The S/N is then used to evaluate the quality characteristics, while ANOVA is applied to analyze important process conditions (Yuin and Alan, 2000). Each combination of control factors for volume, safety factor and maximum stress variations is measured by FEA in the Taguchi experimental design. The S/N ratios are used for optimization of the control factors. A low volume and maximum tensile stress as well as a high safety factor is of great importance in terms of product quality, cost and implant life. Depending on the characteristic type, "the nominal is the best" [equation (1)], "the largest is the best" [equation (2)] and "the smallest is the best" [equation (3)] are used to give the objective function (Masmiati and Sarhan, 2015).

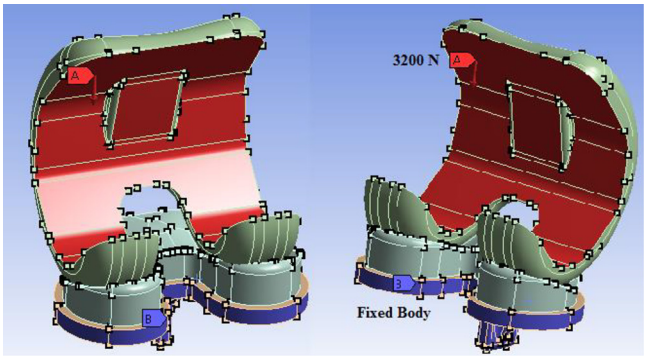

Figure 6.
FEA assembly design

$$\text{Nominal is best: } \frac{S}{N} = 10\log\left(\frac{-y}{S_y^2}\right) \quad (1)$$

$$\text{Largest is best: } \frac{S}{N} = -\log\left(\frac{1}{n}\sum_{i=1}^{n}\frac{1}{y_i^2}\right) \quad (2)$$

$$\text{Smallest is best: } \frac{S}{N} = -\log\left(\frac{1}{n}\sum_{i=1}^{n}y_i^2\right) \quad (3)$$

Here, η is the S/N, yi is the ith test response data result, and n is the ith test repeated number. In the Minitab program, for each experiment, equations were used to calculate the S/N ratios (Minitab Corp., 2010; Nas and Öztürk, 2018; Chen *et al.*, 2010).

4.2.3 Step 3: determination of optimum design levels required to obtain minimum volume and maximum safety factor. In this step, the safety factor and volume variations for the varying maximum stress areas determined by the ANOVA results were listed in the table for each experimental design parameter. It was also necessary to calculate the F force per cent ratio for each experimental design parameter (Figure 7). Stress analysis results showed maximum stress in two different areas (Figure 8). These were the two areas that were fractured as reported by Wada et al. and Luring *et al.* (Figure 1) (Luring *et al.*, 2007; Wada *et al.*, 1997). The parameters were determined separately, and the effect types were grouped

	P1	P2	P3	P4	P5	P6	P7	P8	P9	P10	P11	P12	P13	P14	P15	P16	P17	P18
1st Area Safety Factor	0.19	0	0.31	2.05	1.17	5.79	7.24	1.32	0.25	0.22	0.08	0.85	0.08	10.4	20.84	1.04	0.31	1.21
F% Effect	0.36	0.00	0.58	3.85	2.20	10.89	13.61	2.48	0.47	0.41	0.15	1.60	0.15	19.59	39.18	1.96	0.58	2.27
2nd Area Safety Factor	4.34	22.66	164	9.4	0.69	0.48	7.81	5.87	0.61	0.22	0.17	0.7	0.43	8.03	20.75	2.99	0.43	0.03
F% Effect	1.74	9.09	65.60	3.77	0.28	0.19	3.13	2.35	0.24	0.09	0.07	0.28	0.17	3.22	8.32	1.20	0.17	0.01
Volume	0.87	6.45	0.38	0.36	3.92	110.4	254.7	0.02	0.43	1.2	1.93	4.37	8.88	216	405.8	4.3	241	40.3
F% Effect	0.07	0.49	0.03	0.03	0.30	8.39	19.36	0.00	0.03	0.09	0.15	0.33	0.67	16.44	30.84	0.33	18.32	3.06

Figure 7.
ANOVA results for the safety factor and volume variation (F%) impact intensity

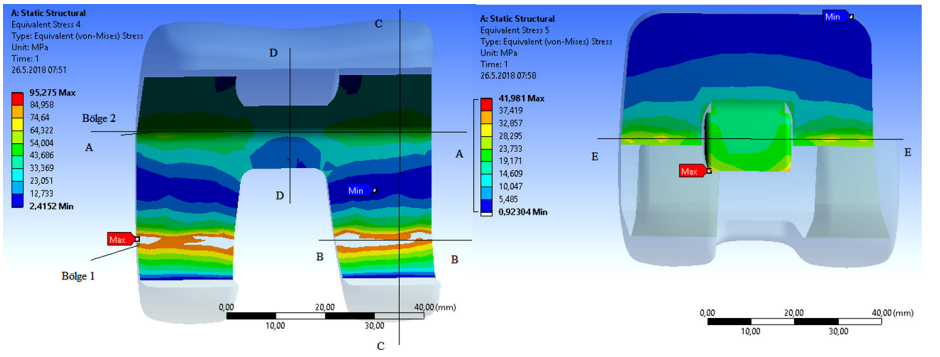

Figure 8.
Section lines and areas of varying maximum stress

as strength and volume results (Figure 9). For example: the changes in the levels of the parameters marked by the green (P_1, P_2, P_3) increase the safety coefficient in the 2nd area, while these changes affect the volume of the design at a much lower rate (Figure 7). The changes in the levels of the parameters marked in red (P_4, P_8, P_{12}, P_{16}) increase the safety factor in both stress areas when keeping the volume amount of the geometry low. The parameters marked with yellow (P_6, P_7, P_{14}, P_{15}, P_{17}, P_{18}) are the parameters that affect the volume amount and the safety factor values to the same extent.

4.3 Obtaining design geometry for defined conditions

In this last proposed step for optimization of industrial design, the relationship between the safety factor value and the volume was examined in a new way. The criteria used in this method differed from the methods in the literature used to evaluate ANOVA results and S/N ratios. To examine these values, some conditions were defined. In the last step of this stage, a map was created showing the stress distribution on the surfaces with the maximum amount of stress. Stress distribution maps of the three-dimensional models were generated by evaluating the sections. It was proposed that if the difference in the stress variation in all sections of a design showed linear results, then that design geometry would have a minimum volume value.

Step 1: defining the optimum design conditions

When selecting these design parameters, the S/N ratios in Figure 10 were compared with the ANOVA results. To optimize the design, it was necessary to select parameter levels according to different criteria. Four different design geometries were selected, including minimum volume, maximum safety factor, maximum safety factor and minimum weight, and maximum safety factor and average weight. Each condition was evaluated according to the ANOVA results in (Figure 7).

1st condition: for minimum volume

The smallest volume was chosen ("the smallest is best") according to the S/N graphs calculated for the volume. However, parameters 8 and 11 were equal at two levels. Considering the S/N graph, the 1st area safety factor was selected for these two equal levels (Table IV).

2nd condition: for maximum safety factor

Because the minimum safety factor was formed in the 1st area, the safety factor was chosen for "the largest is best" according to the calculated S/N graphs in this region. However, it was observed that half of the parameters were equal at two levels. Considering the S/N graph, the 2nd area safety factor was selected for these two equal levels.

3rd condition: for maximum safety factor and minimum volume

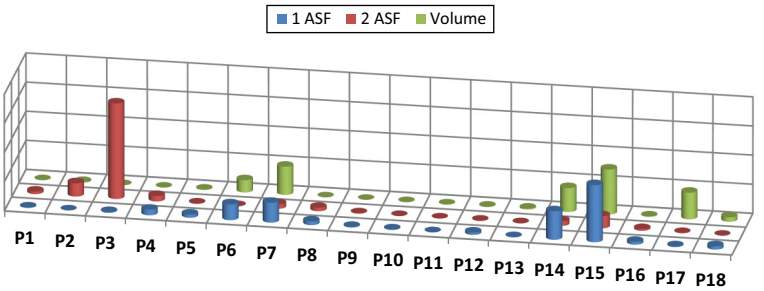

Figure 9.
Effects of all parameters on stress and volume changes

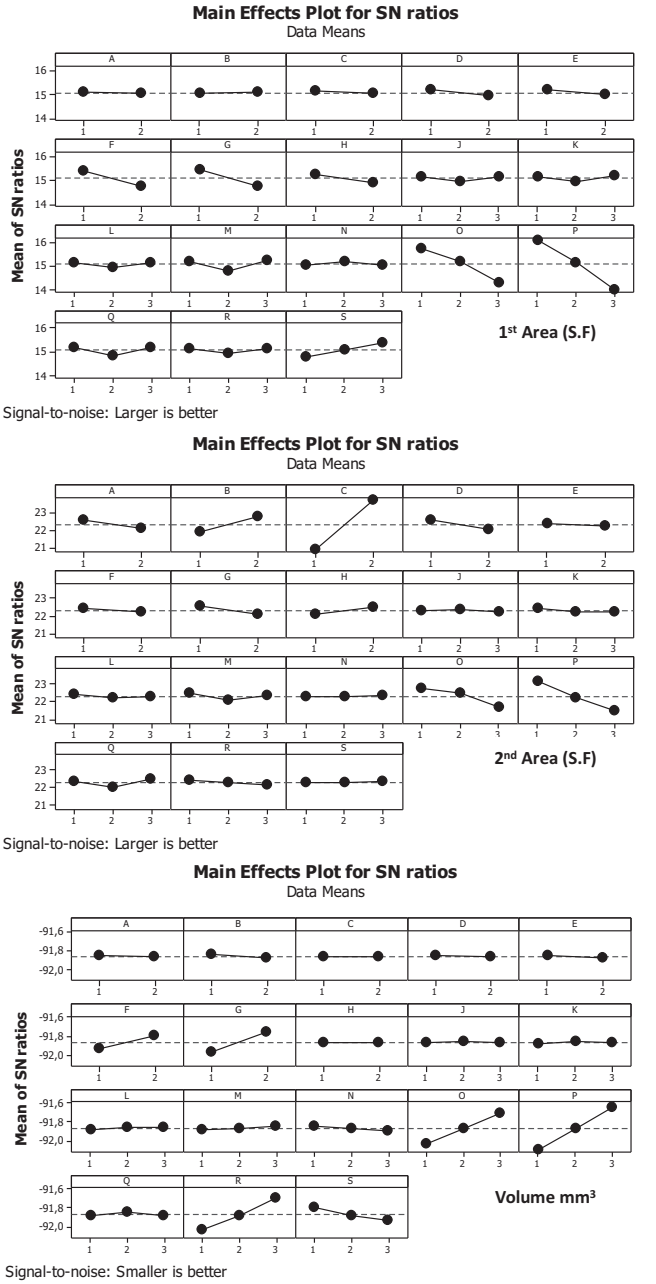

Figure 10.
Taguchi S/N ratios for the safety factor and volume variation

The 1st and 2nd areas were expected to be close to the maximum safety factor however, the volume was selected to be close to the minimum (red and green parameters). In addition, the minimum weight was selected for the 6th, 7th, 14th, 15th, 17th and 18th parameters (yellow parameters).

4th condition: for maximum safety factor and approximately average volume

As the 1st area needed to be a close to the maximum safety factor, the volume was determined as average. While making these choices, parameter levels were established by taking the ANOVA variations into consideration. These levels were determined by examining the percentile variations of the 6th, 7th, 14th, 15th, 17th and 18th parameters (yellow parameters). The parameters that affected a high volume ratio (per cent) were selected as low. Parameters with a safety factor greater than the volume ratio were selected as average or the lowest according to the weight ratio (Table V).

Step 2: creation of surface stress maps for comparison of different conditions

Depending on the selected criteria, the same stress variations could not be expected on all surfaces of the design geometries for different parameter levels. In classical calculations, in this step only the stress variations that are shown as color changes would be given on a surface stress map graph (Harrysson *et al.*, 2007; Kumar and Sarkar, 2018; Villa *et al.*, 2004). Thus, an evaluation could be made along the whole surface line considered to be the maximum stress. To compare the optimum designs for the five different sections in the analysis results, graphics were prepared showing the varying amounts of stress (Figure 8).

Step 3: deciding on optimal design geometry

Verification tests were performed for the results obtained in the last step of this model. Thus, it was possible to determine the accuracy of the methods used in this model. Afterwards, the results of the surface stress distribution maps were examined and compared. In this study, the effects of the Minitab program Predict Taguchi Result feature on the safety factor and volume variations for the selection of the four different criteria were evaluated by analyzing the same FEM features (Table IV). Thus, this numerical estimation could be compared with the FEA (Table VI).

5. Results and discussion

The S/N ratios for the volume, maximum stress and safety factor of each parameter were calculated by Taguchi analysis (Figure 10). Thus, the effects of each design parameter level on the safety factor and volume variation were investigated. This graph was created for the two different areas where the maximum stress was specified in Figure 8. In Table III, the results of the FEM analysis of all DOE are shown compared with maximum stress, safety factor calculation and volume variations for the two different areas where maximum stresses occurred. The results of ANOVA for the two different maximum stress area safety factor and volume variations are listed in (Figure 7) for each experimental design parameter. In addition, the F force per cent rate was calculated for each experimental design parameter. In addition, the graph of the rate of the effect of the design parameter levels on the maximum stress amount and volume changes in both areas is shown in Figure 10. While making these design parameters, the S/N ratios were compared with those of ANOVA. When optimizing a design, it is necessary to select parameter levels according to different criteria (Step 1: defining the optimum design conditions). Four different design geometries were selected, including minimum volume, maximum safety factor, maximum safety factor for minimum weight and maximum safety factor for average weight. The criteria and parameter levels selected for the 4th condition are shown in Table V (Tables III to VI).

According to the Taguchi analysis (Figure 10) and FEA validation analysis for the four different conditions (Table VI), the stress variations for cross-sections of the five different

Table III.
Taguchi L36 (28 × 38) experimental design and analysis results

No.	1	2	3	4	5	6	7	8	9	10	11	12	13	14	15	16	17	18	$Area_1$ safety factor	$Area_2$ safety factor	$Area_1$ max. stress (MPa)	$Area_2$ max. stress (MPa)	Volume (mm^3)
1	1	1	1	1	1	1	1	1	1	1	1	1	1	1	1	1	1	1	8.2	14	74.1	43.6	42218
2	1	1	1	1	1	1	1	1	2	2	2	2	2	2	2	2	2	2	6.4	11.1	95.2	54.8	39606
3	1	1	1	1	1	1	1	1	3	3	3	3	3	3	3	3	3	3	6.2	10.2	98.6	59.5	37731
4	1	1	1	1	1	2	2	2	1	1	1	1	2	2	2	2	3	3	5.5	11.4	109.9	53.3	38019
5	1	1	1	1	1	2	2	2	2	2	2	2	3	3	3	3	1	1	3.6	9	132.2	67.4	36936
6	1	1	1	1	1	2	2	2	3	3	3	3	1	1	1	1	2	2	6.3	12.8	95.7	47.5	39859
7	1	1	2	2	2	1	1	1	1	1	2	3	1	2	3	3	1	2	5.3	14.3	114.9	42.7	39559
8	1	1	2	2	2	1	1	1	2	2	3	1	2	3	1	1	2	3	6	14.7	100.6	41.5	40729
9	1	1	2	2	2	1	1	1	3	3	1	2	3	1	2	2	3	1	5.7	14	106	43.5	39502
10	1	2	1	2	2	1	2	2	1	1	3	2	1	3	2	3	2	1	5	10.8	120.2	56.6	38215
11	1	2	1	2	2	1	2	2	2	2	1	3	2	3	3	1	3	2	5.5	11.5	109.5	53.2	38138
12	1	2	1	2	2	1	2	2	3	3	2	1	3	2	1	2	1	3	6.5	12.9	93.6	47.4	41296
13	1	2	2	1	2	2	1	2	1	2	3	1	3	2	1	3	3	2	6.63	19.5	92.2	31.1	39794
14	1	2	2	1	2	2	1	2	2	3	1	2	1	3	2	2	3	3	5.4	16.6	111.9	36.4	39856
15	1	2	2	1	2	2	1	2	3	1	2	3	2	1	3	2	2	1	5.2	15.6	115.7	38.8	38797
16	1	2	2	2	1	2	2	1	1	2	3	2	1	1	3	2	3	3	5.1	13.8	118.8	44.1	37368
17	1	2	2	2	1	2	2	1	2	3	1	3	2	2	1	3	1	1	6.4	18.7	99.9	32.3	39871
18	1	2	2	2	1	2	2	1	3	1	2	1	3	3	2	1	2	2	5	14.9	120.9	40.7	37967
19	2	1	2	2	1	1	2	2	1	2	1	3	3	3	1	2	2	1	5.4	14	112.2	43.6	38931
20	2	1	2	2	1	1	2	2	2	3	2	1	2	1	2	3	3	2	6.1	14	99.7	43.6	38992
21	2	1	2	2	1	1	2	2	3	1	3	2	2	2	3	1	1	3	5.2	12.7	115.9	48.1	39054
22	2	1	2	2	1	2	2	1	1	2	2	3	3	1	2	1	1	3	6.3	14.6	96.5	41.8	40283
23	2	1	2	2	1	2	2	1	2	3	3	1	1	2	3	2	2	1	4.6	12.5	135.5	48.7	36922
24	2	1	2	2	1	2	2	1	3	1	1	2	2	3	1	3	3	2	5.7	13.9	106.7	43.9	38146
25	2	1	1	2	2	2	1	2	1	3	2	1	2	3	3	1	3	1	4.6	9.1	130	67	36622
26	2	1	1	2	2	2	1	2	2	1	3	2	3	1	1	2	1	2	6.4	12.6	95.3	48.3	42057
27	2	1	1	2	2	2	1	2	2	2	1	3	1	2	2	3	2	3	5.8	10.7	104.6	57.1	39455
28	2	2	2	1	1	1	1	2	1	3	2	2	2	1	1	3	2	3	7.4	20.4	82.2	29.9	42100
29	2	2	2	1	1	1	1	2	2	1	3	3	3	2	2	1	3	1	6.1	18.1	99	33.7	38841
30	2	2	2	1	1	1	1	2	3	2	1	1	1	3	3	2	1	2	4.9	15.1	124	40.3	38916
31	2	2	1	2	1	2	1	1	1	3	3	3	2	3	2	2	1	2	5.3	9.3	114.9	65.5	39293
32	2	2	1	2	1	2	1	1	2	1	1	1	3	1	3	3	2	3	5.7	11.2	107	54.4	39860
33	2	2	1	2	1	2	1	1	3	2	2	2	1	2	1	3	2	1	6.1	11.4	99.6	53.5	39352
34	2	2	1	1	2	1	2	1	1	3	1	2	3	2	3	1	2	2	5	10.2	121.3	59.6	38675
35	2	2	1	1	2	1	2	1	2	1	2	3	1	3	1	2	3	3	5.8	11.2	104.4	54.2	38511
36	2	2	1	1	2	1	2	1	3	2	3	1	2	1	2	3	1	1	6.2	12.5	98.3	48.4	40425

regions are given in the order of comparison in Figures 11-15. Figure 11 shows variations in stress after surface area number seven (C7). In the area to the left of C7, the stress amount for the 1st condition was at the maximum, whereas for the 2nd condition, the amount of stress decreased significantly. In addition, in the surface areas on the right side, the 3rd condition was subjected to less stress and the safety factor design was determined to be the highest in this section.

When the maximum variation of stress for the B-B section is examined (Figure 12), the 3rd and 2nd conditions gave a more linear result than the others. Fluctuations in the amount of stress were observed for the 1st and 4th conditions depending on the surface shapes. Except for the 3rd condition, in the 1st and 4th conditions, the safety factor was higher for this section.

The C-C section in Figure 13 provides an insight into how cross-sectional surface areas, depending on their transitions, can affect the amount and areas of stress variation. Regarding the safety factor, the 2nd and 4th conditions were safer when compared to the others. When the ratio of volume to safety factor was taken into consideration, the 4th condition may have been more favorable. At the same time, depending on the 1st and 3rd conditions, the amount of stress in different regions varied according to the regional results of the design parameters.

As shown in Figure 14, maximum stress amounts varied in two different parts. This is considered to be a flag design because the stress amount for the four different design options varies according to different volume changes in the other surface areas where the flag is located.

Trial no.	1	2	3	4	5	6	7	8	9	10	11	12	13	14	15	16	17	18
01	1	1	2	1	1	2	1	(1)-2	2	2	1-3	3	1	3	3	2	3	1
02	1	2	1	1	1	1	1	1	(1)-3	(1)-3	(1)-3	(1)-3	2	(1)-3	(1)-3	1-(3)	(1)-3	3
03	1	2	1	1	1	2	2	1	1	3	1	3	2	3	3	1	3	1
04	1	2	1	1	1	1	2	1	1	3	1	3	2	2	3	1	3	3

Table IV. Parameter levels specified for four different conditions

Parameters	P_6	P_7	P_{14}	P_{15}	P_{17}	S_{18}
1st area safety factor	10.89	13.61	19.59	39.18	0.58	2.27
Volume	8.39	19.36	16.44	30.84	18.32	3.06
Selection	*Safety factor maximum*	*Weight lowest*	*Weight average*	*Weight lowest*	*Weight lowest*	*Security factor maximum*
Level	1	2	2	3	3	3

Table V. ANOVA results for safety factor and volume variation (F%) impact intensity

Trial no.	Volume	1st area safety factor	2nd area safety factor	1st area max. stress	2nd area max. stress
01	36113	5.3	9.8	114.6	62.2
02	42839	8.2	14.7	74.5	42
03	35598	4.9	8.2	124	51.3
04	37308	5.8	10.1	107.3	60.8
Average error (%)	*1*	*3.3*	*16.9*	*2.6*	*6.2*

Table VI. FEM validation analysis

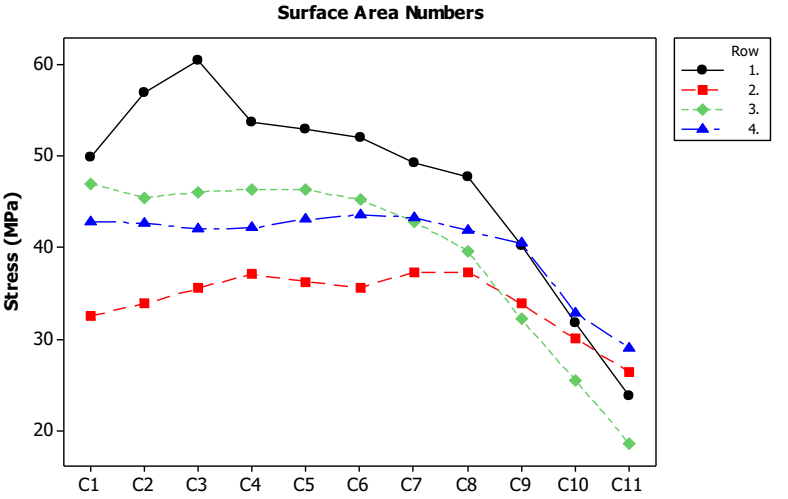

Figure 11.
Varying stress (MPa) for cross-section A-A

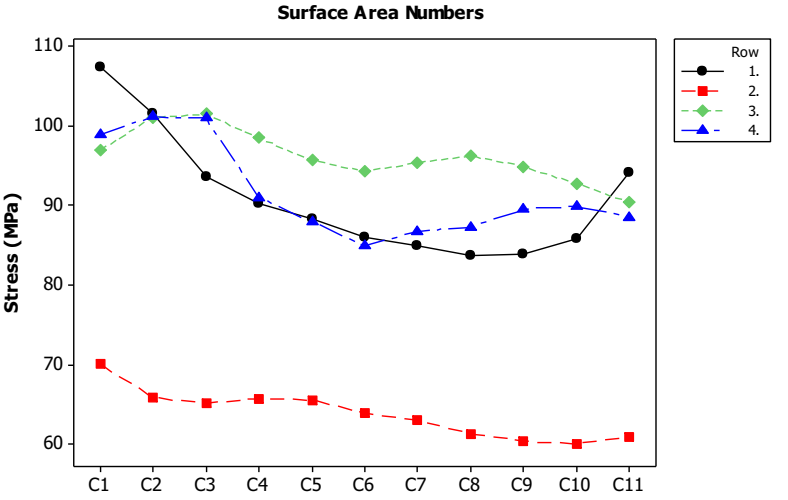

Figure 12.
Varying stress (MPa) for cross-section B-B

The surface stress distribution map for the E-E section is given in Figure 15. In this section, as in the D-D section and in contrast to the other sections, minimum stress was observed for the 2nd and 3rd conditions. This revealed that the 3rd condition on the surface of the inner flange would provide more strength than the 4th condition.

Two different fracture areas were reported by Wada *et al.* and Luring *et al.* (Luring *et al.*, 2007; Wada *et al.*, 1997). Therefore, it is very important to ensure the maximum safety factor in these two regions. The minimum design weight and maximum safety factor could be selected in the 4th condition. In this way, optimum design parameters were selected, and optimization of the design geometry was achieved.

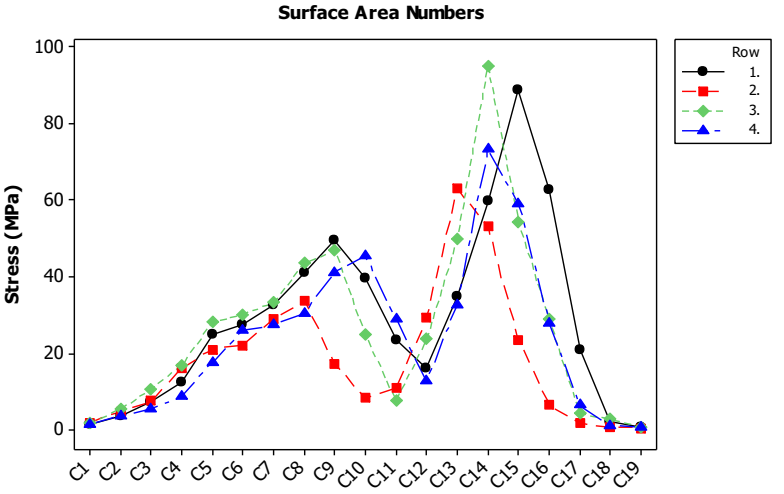

Figure 13.
Varying stress (MPa) for cross-section C-C

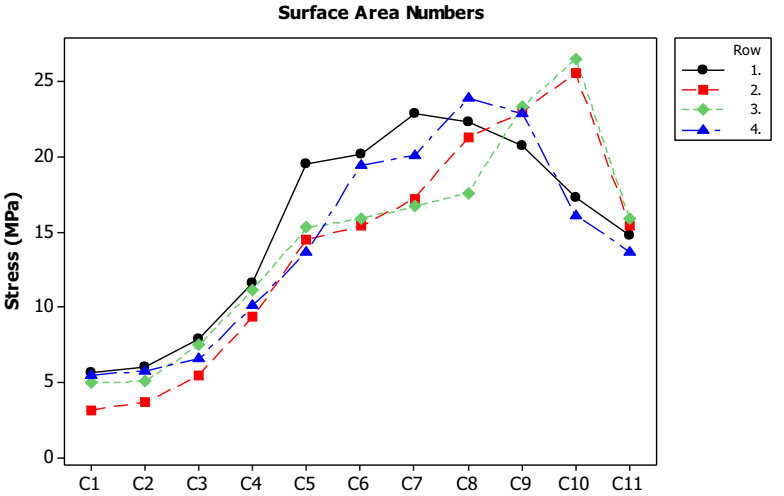

Figure 14.
Varying stress (MPa) for cross-section D-D

Consequently, stress distribution maps were developed for optimum design choices and different designs were developed. Some models have been presented in literature dealing with optimization of design and material selection and process modeling of FEA studies (Ilzarbe *et al.*, 2008; Harrysson *et al.*, 2007; Sanecki and Zieliński, 2006). Using FEA and RSM, Bahraminasab *et al.* performed a multi-purpose design optimization for a FGM femoral component (Bahraminasab *et al.*, 2014a). By using various geometric and material combinations, Kumar and Sarkar drew a flux diagram illustrating the optimization process for TKP design characteristics and materials (Kumar and Sarkar, 2018). In this study, for the first time in the literature and as distinct from classical analysis calculations, a process which provides optimization in design has been presented by examining the effects of

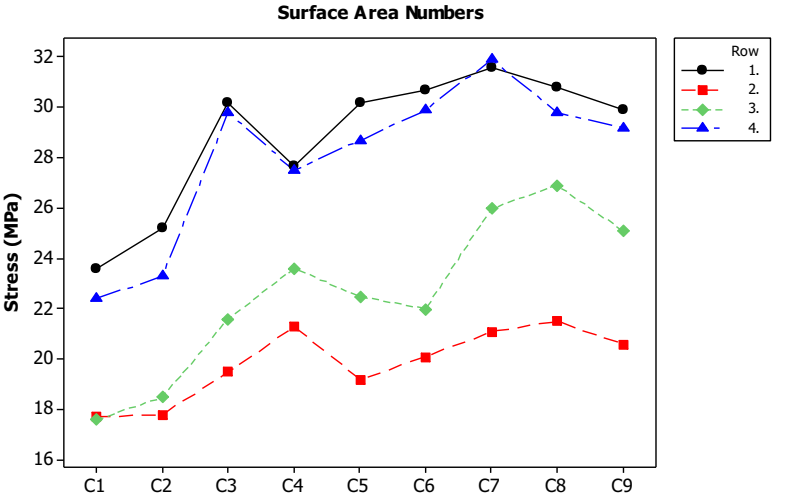

Figure 15.
Varying stress (MPa) for cross-section E-E

design parameters on strength and volume variations. In addition, validation was done by using FEA, and the results were verified using statistical methods. We took advantage of the ANSYS FEM Program and Taguchi method in this study, in which we investigated the optimization of a TKP industrial design. All strength calculation methods can be used together with all statistical methods in this proposed design development process model. The most probable cause of TKP failure was reported to be the thinness of the metal in this design area (Wada *et al.*, 1997). In addition, the sharp bend and thin metal (4 mm) in the design were constantly exposed to continuous loads resulting in regions of high stress concentration (Luring *et al.*, 2007).

When patient status reports were examined, it was understood that the industrial design geometries were not shaped according to specific criteria. This study sought to eliminate these problems related to breakage by presenting a new design optimization model. Parameters not affecting the strength which had unnecessary weight were determined. Design errors were prevented by using the parameter levels selected in patient status reports according to the statistical method. Villa *et al.*, by applying FEM analysis, stated that the maximum stress would occur at a 45° angle, and proved this via experimental studies (Villa *et al.*, 2004). We used the FEM conditions in these studies and observed that there were maximum stresses at the two different areas where fractures were reported by Luring *et al.* (2007) and Wada *et al.* (1997). Results proved that the fractures reported as occurring in these regions were under dynamic load at a 40-50° angle in patients using the TKP. Therefore, an optimization was made for an industrial design by taking into account the maximum stress variation in these two regions.

The SFV in the 1st area were affected by P_{15} (39.1 per cent), P_{14} (19.5 per cent) and P_7 (13.6 per cent). In the 2nd area, the SFV were affected by P_3 (65.6 per cent), P_2 (9 per cent) and P_{15} (8.3 per cent). Different parameters in both regions affected these results at different rates. The volume was significantly affected by P_{15}, P_7 and P_{14} parameters. It was determined that these parameters affected the safety factor the most in the 1st area. The parameters affecting the safety factor in the 1st area at the highest rate while increasing the volume to a minimum were P_4, P_8, P_{12} and P_{16}. Considering that patients may use a TKP for fifteen years, the minimum weight value is very important and must be maintained along

with the maximum safety value. The effects of strength characteristics were calculated by using the Minitab Program Predict Taguchi Results feature for four different selections (Table IV). Thus, these numerical predictions could be compared with the FEM analysis (Table VI). With this new design development model, it was possible to estimate strength and volume variations with high accuracy. The FEA results showed that the minimum weight was provided for the 3rd condition parameter options, while the safety factor was also the minimum in this option. Table VII shows the variation in volume and safety factor as a percentage of the other conditions.

6. Conclusion

In the literature, design errors have been reported in patient status reports related to knee prostheses (Borus and Thornhill, 2008; Luring *et al.*, 2007; Wada *et al.*, 1997; Cameron and Welsh, 1990; Sandborn *et al.*, 1987). In addition, optimization studies related to this subject are included in the literature (Bahraminasab *et al.*, 2014a; Bahraminasab *et al.*, 2014b; Harrysson *et al.*, 2007; Chandran *et al.*, 2009; Huang *et al.*, 2017; Willing and Kim, 2009). In this article, the optimum loading conditions of a prosthesis are taken into consideration and optimum levels are investigated (Villa *et al.*, 2004). This optimization study was achieved with a new method. A safety factor value of 5.73 was obtained for the volume of 39,219 mL for a region which had maximum stress. For a maximum safety factor and at the same time an average weight, values of 37,308 mL and 5.8 for volume and safety factor were obtained, respectively, using statistical methods. However, in the proposed new model which had 36 different experimental designs according to determined criteria, this safety factor value could not be obtained for a lesser volume at any parameter. The maximum safety factor in the 1st and 2nd areas was calculated as 8.2 and 14.7, respectively, according to the calculation made by considering the 2nd condition. In this study, the proposed parametric design model was able to calculate safety coefficient values at 89.9 per cent and maximum stress calculations at 95.6 per cent accuracy. As a result of this study, it was found that the optimum design parameter level could only be selected for the specified criteria. In the case of materials whose weight is expected to be minimum, the selection should be made for an average weight but for a maximum safety factor. In addition, in design development work using the classic FEA; however, it was observed that it is a mistake to only consider the importance of maximum stress. The stress distribution graphs of all the sections where stress occurs must be examined. This proposed industrial product design optimization process was applied to TKP models. However, this method can be enhanced to develop a technique capable of providing high accuracy optimization for all designs. With this article, design parameters in the literature can provide an answer to the desired design criteria, unlike the methods which are not associated with design elements. Thus, this study can contribute to the literature as a reference that can be applied to all universal industrial design optimization studies.

Trial no.	Volume	1st area safety factor	2nd area safety factor
03	35,598	4.9	8.2
01 (%)	1.5	7.5	6.4
04 (%)	4.6	15.6	19.9
02 (%)	17	41	45

Table VII. Volume % and SFV of experimental groups

References

Bahraminasab, M., Sahari, B.B., Edwards, K.L., Farahmand, F., Hong, T.S., Arumugam, M. and Jahan, A. (2014a), "Multi-objective design optimization of functionally graded material for the femoral component of a total knee replacement", *Materials and Design*, Vol. 53, pp. 159-173.

Bahraminasab, M., Sahari, B.B., Edwards, K.L., Farahmand, F., Jahan, A., Hong, T.S. and Arumugam, M. (2014b), "On the influence of shape and material used for the femoral component pegs in knee prostheses for reducing the problem of aseptic loosening", *Materials and Design*, Vol. 55, pp. 416-428.

Boran, S., Hurson, C., Synnott, K. and Keogh, P. (2005), "Biomechanical analysis of tibial tray fractures post total knee arthroplasty", *European Journal of Orthopaedic Surgery and Traumatology*, Vol. 15, pp. 295-299.

Borus, T. and Thornhill, T. (2008), "Unicompartmental knee arthroplasty", *Journal of the American Academy of Orthopaedic Surgeons*, Vol. 16 No. 1, pp. 9-18.

Cameron, H.U. and Welsh, R.P. (1990), "Fracture of the femoral component in unicompartmental total knee arthroplasty", *Journal of Arthroplasty*, Vol. 5 No. 4, pp. 315-317.

Chandran, N., Amirouche, F., Gonzalez, M.H., Hilton, K.M., Barmada, R. and Goldstein, W. (2009), "Optimisation of the posterior stabilised tibial post for greater femoral rollback after total knee arthroplasty – a finite element analysis", *International Orthopaedics*, Vol. 33 No. 3, pp. 687-693.

Chen, W.L., Huang, C.Y. and Hung, C.W. (2010), "Optimization of plastic injection molding process by dual response surface method with nonlinear programming", *Engineering Computations*, Vol. 27 No. 8, pp. 951-966, available at: https://doi.org/10.1108/02644401011082971

Dai, Y., Scuderi, G.R., Penninger, C., Bischoff, J.E. and Rosenberg, A. (2014), "Increased shape and size offerings of femoral components improve fit during total knee arthroplasty", *Knee Surgery, Sports Traumatology, Arthroscopy*, Vol. 22 No. 12, pp. 2931-2940.

Harrysson, O.L.A., Hosni, Y.A. and Nayfeh, J.F. (2007), "Custom-designed orthopedic implants evaluated using finite element analysis of patient-specific computed tomography data: femoral-component case study", *BMC Musculoskeletal Disorders*, Vol. 91, pp. 1-10.

Huang, C.H., Hsu, L.I., Chang, T.K., Chuang, T.Y., Shih, S.L., Lu, Y.C., Chen, C.S. and Huang, C.H. (2017), "Stress distribution of the patellofemoral joint in the anatomic V-shape and curved dome-shape femoral component: a comparison of resurfaced and unresurfaced patellae", *Knee Surgery, Sports Traumatology, Arthroscopy*, Vol. 25 No. 1, pp. 263-271.

Ilzarbe, L., Alvarez, M.J., Viles, E. and Tanco, M. (2008), "Practical applications of design of experiments in the field of engineering: a bibliographical review", *Quality and Reliability Engineering International*, Vol. 24 No. 4, pp. 417-428.

Insall, J. and Aglietti, P.A. (1980), "Five to seven-year follow-up of unicondylar arthroplasty", *Journal of Bone and Joint Surgery*, Vol. 62 No. 8, pp. 1329-1337.

Kibar, M.E., Ozcan, O., Dusova-Teke, Y., Yonel, G.E. and Akin, A.N. (2016), "Optimization, modeling and characterization of sol-gel process parameters for the synthesis of nanostructured boron doped alumina catalyst supports", *Microporous and Mesoporous Materials*, Vol. 229, pp. 134-144.

Küçük, Ö., Öztürk, B. and Varhan, S. (2017a), "Investigation of the design parameters affecting the safety factor in fittings by using Taguchi method", *The Turkish Journal of Occupational/Environmental Medicine and Safety: The 2nd international Water and Health Congress -Issue: The 2nd international Water and Health Congress*, ISSN: 2149-4711, p. 10.

Küçük, Ö. and Öztürk, B. (2017b), "Development of design geometry of aluminum fittings for healthy and safety sanitary installations", *Journal of Environmental Protection and Ecology*, Vol. 18-2, pp. 776-787.

Kumar, T.S. and Sarkar, D. (2018), "Computer-aided design, finite element analysis and material-model optimisation of knee prosthesis", *Journal of the Australian Ceramic Society*, Vol. 54 No. 3, pp. 429-438.

Laskin, R.S. (1978), "Unicompartmental tibiofemoral resurfacing arthroplasty", *Journal of Bone and Joint Surgery*, Vol. 60 No. 2, pp. 182-185.

Luring, C., Perlick, L., Schubert, T. and Tingart, M. (2007), "A rare cause for knee pain: fracture of the femoral component after TKR. A case report", *Knee Surgery, Sports Traumatology, Arthroscopy: Official Journal of the Esska*, Vol. 15 No. 6, pp. 756-757.

Masmiati, N. and Sarhan, A.A.D. (2015), "Optimizing cutting parameters in inclined end milling for minimum surface residual stress – Taguchi approach", *Measurement*, Vol. 60, pp. 267-275.

Minitab Corp (2010), "Minitab User Manual Release 16.2, making data analysis easier", Minitab Corp.

Minnoye, S.L.M. and Plettenburg, D.H. (2009), "Design, fabrication, and preliminary results of a novel below-knee prosthesis for snowboarding: a case report", *Prosthetics and Orthotics International*, Vol. 33 No. 3, pp. 272-283.

Nas, E. and Öztürk, B. (2018), "Optimization of surface roughness via the Taguchi method and investigation of energy consumption when milling spheroidal graphite cast iron materials", *Materials Testing*, Vol. 60 No. 5, pp. 519-524.

Öztürk, B., Uğur, L., Erzincanlı, F. and Küçük, Ö. (2018), "Optimization of polyethylene inserts design geometry of total knee prosthesis", *International Scientific and Vocational Studies Journal*, Vol. 2, pp. 31-39.

Panousis, K., Murnaghan, C., Koettig, P. and Grigoris, P. (2004), "Fracture of the femoral component of a Brigham unicompartmental knee: a case report", *Knee Surgery, Sports Traumatology, Arthroscopy : Official Journal of the Esska*, Vol. 12 No. 4, pp. 307-310.

Rawal, B.R., Yadav, A. and Pare, V. (2019), "Life estimation of knee joint prosthesis by combined effect of fatigue and wear", *Procedia Technology*, Vol. 23, pp. 60-67.

Ross, P.J. (1996), *Taguchi Techniques for Quality Engineering*, McGraw-Hill, New York, NY.

Sandborn, P.M., Cook, S.D., Kester, M.A. and Haddad, R.J. (1987), "Fatigue failure of the femoral component of a unicompartmental knee", *Clinical Orthopaedics and Related Research*, Vol. 222, pp. 249-254.

Sanecki, H. and Zieliński, A.P. (2006), "Crack propagation modelled by T elements", *Engineering Computations*, Vol. 23 No. 2, pp. 100-123, available at: https://doi.org/10.1108/02644400610644496

Taguchi, G. (1990), *Introduction to Quality Engineering*, Asian Productivity Organization, Tokyo.

Van den Heever, D., Scheffer, C., Erasmus, P. and Dillon, E. (2011), "Method for selection of femoral component in total knee arthroplasty (tka)", *Australasian Physical & Engineering Sciences in Medicine*, Vol. 34 No. 1, pp. 23-30.

Van der Veen, H.C. and Van Raay, J.J. (2014), "Fracture of an Oxford femoral component: a case report", *The Knee*, Vol. 21 No. 1, pp. 325-327.

Vertullo, C.J., Graves, S.E., Peng, Y. and Lewis, P.L. (2018), "An optimum prosthesis combination of low-risk total knee arthroplasty options in all five primary categories of design results in a 60% reduction in revision risk: a registry analysis of 482,373 prostheses", *Knee Surgery, Sports Traumatology, Arthroscopy*, doi: 10.1007/s00167-018-5115-z.

Villa, T., Migliavacca, F., Gastaldi, D., Colombo, M. and Pietrabissa, R. (2004), "Contact stresses and fatigue life in a knee prosthesis: comparison between in vitro measurements and computational simulations", *Journal of Biomechanics*, Vol. 37 No. 1, pp. 45-53.

Wada, M., Imura, S., Bo, A., Baba, H. and Miyazaki, T. (1997), "Stress fracture of the femoral component in total knee replacement: a report of 3 cases", *International Orthopaedics (Orthopaedics)*, Vol. 21 No. 1, pp. 54-55.

Willing, R. and Kim, I.Y. (2009), "Three dimensional shape optimization of total knee replacements for reduced wear", *Structural and Multidisciplinary Optimization*, Vol. 38 No. 4, pp. 405-414.

Yuin, W. and Alan, W. (2000), *Taguchi Methods for Robust Design*, 1st ed., ASME Press, New York, NY.

Corresponding author
Burak Öztürk can be contacted at: burak.ozturk@bilecik.edu.tr